High-resolution photodetachment spectroscopy from the lowest threshold of O^-

Anne Joiner,* Robert H. Mohr,† and J. N. Yukich‡
Physics Department, Post Office Box 7133, Davidson College, Davidson, North Carolina 28035-7133, USA
(Received 30 December 2010; published 8 March 2011)

We conducted photodetachment spectroscopy near the lowest detachment threshold from O^- in a 1-T field with sufficient resolution to observe a magnetic field structure similar to that observed in experiments conducted at the threshold of the electron affinity. These observations included not only cyclotron structure but also, to a smaller degree, individual Zeeman thresholds. The experiment was conducted in a Penning ion trap and with a single-mode, tunable, amplified diode laser. Finally, analysis of our results yielded a measurement of the lowest threshold energy.

DOI: 10.1103/PhysRevA.83.035401 PACS number(s): 32.80.Gc

I. INTRODUCTION

Photodetachment spectroscopy has been used for several decades to examine detachment from negative ions in external electric fields and magnetic fields [1–12]. In each case, the external field causes some portion of the out-going electron wave function to return to the atomic core. In particular, an external magnetic field forces the electron to execute cyclotron motion, giving rise to a periodic structure in the detachment cross section as a function of photon energy. This structure, with uniform spacing equal to the cyclotron frequency, can be understood to result from interference of the outgoing wave function with itself. Several experiments have also resolved a structure in the detachment cross section due to transitions between the various Zeeman states of the ion and the resulting neutral atom [4,5,11]. Some of these experiments were conducted in fields of several tesla in order to resolve visually the Zeeman structure [4]. Prior experiments conducted at 1.0 T failed to resolve visually this structure due to the presence of numerous overlapping transitions, thermal broadening mechanisms [11], and low signal-to-noise ratios [12]. In general, past work in photodetachment spectroscopy in a magnetic field has proven to be largely consistent with the theory of Blumberg, Itano, and Larson (referred to hereafter as BIL) [1–3]. However, several experiments have revealed a clear departure from this theory [4,5,11], motivating a more careful examination of the theory, specifically with regard to the Zeeman transitions.

In a recent article we reported results from spectroscopy near the lowest threshold of S^- [12]. This is the $^2P_{1/2} \rightarrow {}^3P_2$ transition. With laser polarization parallel to the field (π polarization), only four Zeeman transitions are allowed at each cyclotron threshold. The resolution of this S^- experiment was limited by several factors. Due to the relatively large spin-orbit splitting of the ion, any ensemble of S^- ions has a small population in the $^2P_{1/2}$ state as compared to that of the $^2P_{3/2}$ state. Thus, the results were limited by a poor signal-to-noise ratio. Furthermore, the experiment was conducted at 1.0 T, greatly limiting the magnetic field splitting of the Zeeman thresholds.

In this paper we report on a similar experiment conducted to observe the photodetachment spectroscopy of O^- at its lowest threshold (shown as transition B in Fig. 1 of Ref. [12]). As with the S^- work, this experiment is conducted in a Penning ion trap whose long ion storage times permit relatively high precision of energy measurements. However, several factors distinguish this experiment. The O^- ion has a smaller spin-orbit splitting (roughly 177 cm^{-1} as compared to 484 cm^{-1} for S^-). Thus, a thermal ensemble of O^- ions has a larger population in its $^2P_{1/2}$ state, yielding a higher signal-to-noise ratio. Furthermore, we have increased our magnetic field by nearly 40%, yielding increased separation of Zeeman thresholds. We also found that the increased magnetic field greatly reduced the absolute noise level in our apparatus due to an increased storage time in the Penning ion trap (discussed in Sec. III). Our results show highly repeatable structure in the photodetachment spectrum due to both the cyclotron thresholds and the Zeeman thresholds. Numerical fitting of the data to the BIL theory also yields a value for the O^- lowest detachment threshold that is compatible with other recent measurements.

II. THEORY

The BIL theory has been described previously and most recently as it pertains to this experiment in Ref. [12], so we present a summary of it. This experiment uses laser light polarized parallel to the magnetic field (π polarization) to probe near-threshold s-wave photodetachment near the $^2P_{1/2} \rightarrow {}^3P_2$ transition of O^-. The magnetic field constrains the motion of the outgoing electron to quantized cyclotron orbits uniformly spaced by the cyclotron frequency, and it splits the initial and final atomic states into their respective Zeeman sublevels [2,13]. With π-polarized light, each cyclotron transition consists of four possible Zeeman transitions (see Table I of Ref. [12]). These four transitions are the focus of this work and are numerically tabulated in Sec. IV.

The photoelectron is ejected into a one-dimensional continuum with a total energy given by its cyclotron level and its motion along the field (z) axis as $E = \hbar\omega_0 + \hbar\omega_c(n + 1/2) + \frac{p_z^2}{2m}$, where $\hbar\omega_0$ is the field-free threshold energy, n is the principal quantum number, ω_c is the cyclotron frequency, and p_z is the electron's momentum in the continuum [1,2,13]. The four Zeeman transitions which occur with π-polarized light have threshold energies relative to the zero-field threshold given by

$$E_{if} = \mu_B B(g_f m_f + g_e m_e - g_i m_i + 2n + 1), \qquad (1)$$

where μ_B is the Bohr magneton, B is the magnetic field, and the g factors g_f, g_e, and g_i refer to the $^3P_2$ state of the neutral

*joiner.anne@gmail.com
†rmohr@greenseainc.com
‡joyukich@davidson.edu; http://www.phy.davidson.edu/FacHome/jny/welcome.htm

atom, the electron, and the initial state of the ion, respectively. These four thresholds are spread over $(4/3)\mu_B B$ and their corresponding transitions have relative strengths varying only by 50% [12].

Rather than measure absolute cross sections, our experiments measure the fraction of ions surviving laser illumination as a function of photon energy ν. This fraction is given by $F(\nu) = \sum_i f_i e^{-A\sigma_i(\nu)}$, where we sum over all possible initial states. The relative population of the ith initial state is f_i, A is proportional to the total optical flux during the laser interaction time, and $\sigma_i(\nu)$ is the cross section for detachment from the ith initial state. We assume the ions populate the Zeeman sublevels of the $^2P_{1/2}$ state with a Boltzmann distribution. The total cross section at a given photon energy is the sum of partial cross sections for all allowed transitions obeying energy conservation [2]. We account for a possible short-range interaction between the atom and the departing electron by introducing a parameter γ, so that the partial cross section at each threshold is given by $\sigma(k) \propto \frac{4k}{\gamma^2+4k^2}$, where k is the wave number corresponding to the electron's momentum along the continuum z axis [3]. Our numerical algorithm for fitting the BIL model to the data also accounts for thermal broadening effects and produces a measurement of the field-free detachment threshold.

III. EXPERIMENTAL TECHNIQUE

In this experiment we measure the depletion by photodetachment of O^- ions in the presence of a magnetic field of order 1 T. The ions are created and stored in a Penning ion trap, and illuminated by an amplified diode laser. This overall technique is similar to that used in several previous experiments [1,2,10–12].

Our experiments are conducted with ensembles on the order of 10^4 O^- ions. The ions are created in the trap by dissociative attachment to a carrier gas of N_2O at a pressure of roughly 6×10^{-8} Torr [14]. The optimum electron energy for the dissociative attachment is approximately 1.5 eV. The background pressure of the trap system is less than 10^{-10} Torr. We make a relative measurement of the number of ions stored in the trap by driving the ion cloud in a resonant axial motion with a radio frequency voltage on the trap end caps. The resulting image current generated in the trap ring electrode is detected and amplified by a commercial high-frequency lock-in amplifier. The resonant axial driving technique permits us to selectively drive the $^{16}O^-$ ions and ignore the less abundant isotopes [1,2].

The ions are illuminated by a laser as shown in Fig. 1. The laser system consists of a tunable diode laser operating as a master oscillator and a tapered-gain power amplifier operating in a single-pass scheme. The laser system produces a few hundred milliwatts of single longitudinal mode tunable light at 861 nm. The laser wavelength is measured by a commercial wavelength meter to a precision of 0.36 GHz, and the laser mode is monitored by an 8-GHz free spectral range spectrum analyzer. The optical flux is measured by a photodiode and produces a feedback signal to a shutter that allows us to maintain a constant integrated light flux from cycle to cycle of the experiment.

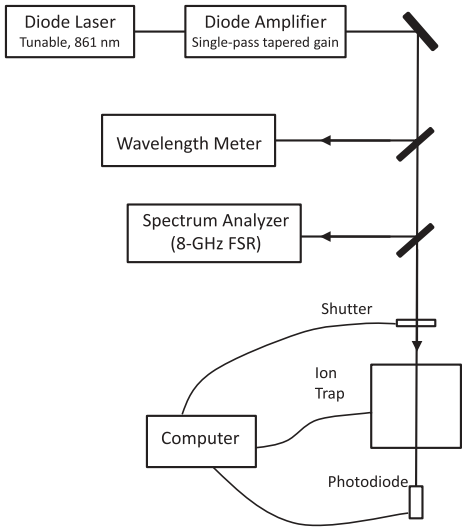

FIG. 1. Schematic diagram of the major optical apparatus and the ion trap. The ions undergo photodetachment with light from a tunable, single-mode, amplified diode laser. A computer-controlled mechanical shutter maintains a constant optical flux, measured by the photodiode, from cycle to cycle of the data acquisition.

The depletion of ions from the trap by photodetachment is determined by making a relative measurement of the number of ions stored in the trap before and after a laser illumination period of roughly 600 ms. The complete data acquisition cycle consists of a background noise measurement, an ion creation period of roughly 8 s, the initial ion trap population measurement, the laser illumination period, and the final trap population measurement. Alternate data cycles measure the trap retention ratio without laser illumination. Thus, we measure an overall fraction of ions surviving laser illumination corrected to first order for background trap losses. We then fit the BIL model to the measured fraction of ions surviving using the adjustable parameters.

In this experiment we encountered the "excess ion" problem with the production of O^- similar to that found in the experiment described in Ref. [12]. Under certain conditions, illumination of the ion cloud with the laser tuned below the lowest photodetachment threshold can produce an apparent increase in the number of trapped O^- ions as measured by the detection system. As a result, the measured fraction of ions surviving detachment can exceed 1.00. In this experiment, the phenomenon may occur as a result of production of NO^- ions by dissociative attachment during the ion production period of the data cycle. While these heavier ions do not contribute any signal to the mass-selective detection system, they may in fact be trapped by the electrostatic potential well. Following simultaneous production of NO^- and O^- during the ion creation period, the subsequent "excess" O^- production is thought to occur as a two-step process during the laser illumination:

$$\begin{aligned} h\nu + NO^- &\rightarrow e^- + NO \\ e^- + N_2O &\rightarrow N_2 + O^-. \end{aligned} \tag{2}$$

The NO^- ion has an electron affinity of approximately 0.026 eV [15], so any NO^- ions illuminated by the laser will be photodetached. The resulting photoelectrons from the first step

have an energy of approximately 1.4 eV, which in turn drives the second step, producing additional O^- ions by dissociative attachment. The net effect below the O^- detachment threshold is to produce a larger cloud of ions during the laser illumination period. We found that this excess ion production was sensitive to the N_2O pressure; reducing the gas pressure diminishes the probability of the above two-step process occurring. We found by reducing the N_2O pressure roughly 30% that we could eliminate the excess ion problem.

In order to improve this experiment's resolution of the four Zeeman transitions over that of Ref. [12], efforts were made to increase the trap magnetic field strength. In addition to improved spectroscopic resolution, we also found greatly improved retention of ions in the trap and greater overall stability of the ion detection signal. These effects both resulted in reduced experimental uncertainties. We attribute these effects to the reduced ion cyclotron orbit radius, which reduces the likelihood of collisions with the N_2O molecules.

IV. RESULTS AND DISCUSSION

In this experiment we collected multiple sets of data to measure the fraction of ions surviving laser illumination as a function of photon energy near the $^2P_{1/2} \rightarrow {}^3P_2$ threshold of O^-. These measurements were made at magnetic fields of 1.0 and 1.36 T. As in the experiment of Ref. [12], we used only π-polarized light in order to limit the number of Zeeman transitions to four and to maximize their resolution. In each experiment the laser bandwidth as measured by the spectrum analyzer was under 200 MHz, which is narrow compared to the other broadening effects such as the motional Stark effect and the Doppler effect. Figure 2 shows an example of the results for $B = 1.36$ T, showing both the overall cyclotron structure as well as repeatable Zeeman structure. Figure 3 shows results

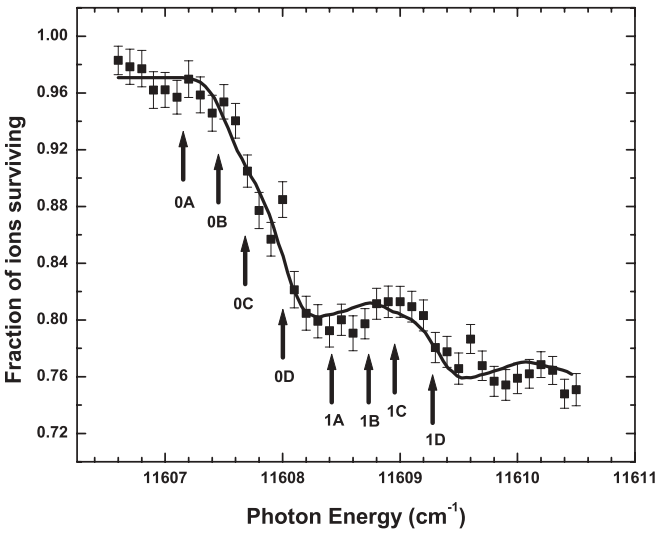

FIG. 2. Photodetachment data at the $^2P_{1/2} \rightarrow {}^3P_2$ threshold of O^-. The percent of ions surviving laser illumination is plotted as a function of photon energy. The data shown are for a field of 1.36 T and π-polarized light. The solid curve shows a fit to the data, from which is derived a measure of the field-free detachment threshold. Labeled arrows show the expected locations of the Zeeman transitions as indicated in Table I.

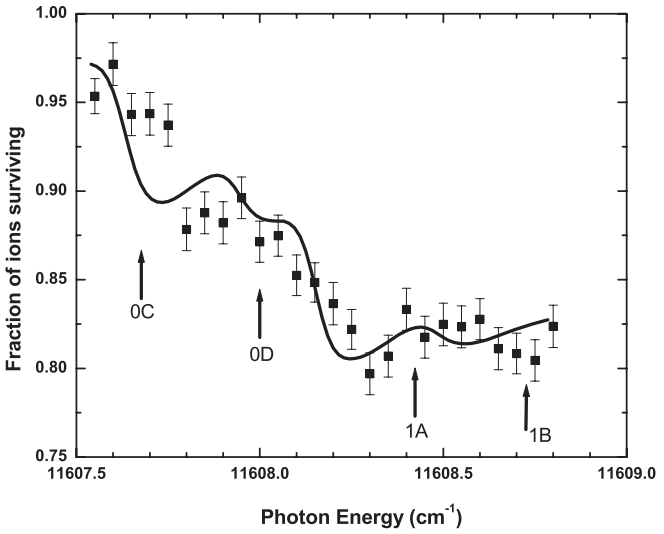

FIG. 3. Photodetachment data at the $^2P_{1/2} \rightarrow {}^3P_2$ threshold taken at higher energy resolution, with $B = 1.36$ T and using π-polarized light. The solid curve shows a fit to the data, and the labeled arrows show the locations of the expected Zeeman thresholds.

from a higher-resolution data set which focuses on the $n = 0$ cyclotron threshold, also for 1.36 T. Each figure includes a theoretical fit of the BIL model to the data. Long-term fluctuations in the ion trap conditions limit the feasible time scale of data acquisition and thus our experiments focus on near-threshold detachment where the magnetic field structure is most prominent.

The BIL theoretical model is fit to each of the individual data sets according to the description in Sec. II. Each theoretical fit yields a measurement and an uncertainty for the field-free detachment threshold. By combining the results from seven separate data sets in a weighted average, we arrive at a value for the lowest O^- detachment threshold of 11607.575(28) cm^{-1}. With the approach taken in Ref. [12], the total uncertainty is composed of three contributions. The overall uncertainty from the theoretical fits is 0.004 cm^{-1}. An absolute experimental uncertainty to three standard deviations from the wavelength meter contributes 0.012 cm^{-1}. And finally, we allow for some possible systematic error in the magnetic field, which is measured to within 0.01 T. By allowing for this uncertainty in the model fitting procedure, we find an additional uncertainty of 0.012 cm^{-1}. For a maximum possible uncertainty we assume no overlap of these contributions, yielding a full confidence interval of 0.028 cm^{-1}. Our value for the lowest detachment threshold is compatible with measurements produced by the photodetachment microscope method: 11784.676(7) cm^{-1} for the O^- electron affinity [16] and 177.09(2) cm^{-1} for the fine-structure splitting $\Delta E(^2P_{1/2} \rightarrow {}^3P_2)$ [17].

In Fig. 2 we see the initial cyclotron threshold as well as the $n = 1$ and $n = 2$ cyclotron structure. Each cyclotron threshold is composed of the four allowed Zeeman thresholds. For a field of 1.36 T, the average spacing between these thresholds is 0.282 cm^{-1}. The Zeeman thresholds are found by evaluating Eq. (1) for the first three cyclotron levels, relative to the experimental measurement of the zero-field $^2P_{1/2} \rightarrow {}^3P_2$ threshold stated above. Thus, by fitting the BIL model to the data, we can determine the expected Zeeman threshold

TABLE I. Details of the allowed Zeeman transitions between the sublevels of $^2P_{1/2}$ in O^- and $^3P_2$ in neutral ***O*** using π-polarized light and a field of 1.36 T. The first two columns give the energy shift in units of $\mu_B B$ and cm^{-1}, respectively, relative to the zero-field threshold. The third column gives the relative weight factor. The last three columns give the expected energies of the Zeeman thresholds for the first three cyclotron levels.

ΔE_{if} (units of $\mu_B B$)	Δ (cm^{-1})	Weight	$n = 0$	$n = 1$	$n = 2$
$-\frac{2}{3}$	−0.423	6	11607.152(0*A*)	11608.422(1*A*)	11609.692(2*A*)
$-\frac{1}{6}$	−0.106	4	11607.469(0*B*)	11608.739(1*B*)	11610.009(2*B*)
$\frac{1}{6}$	0.106	6	11607.681(0*C*)	11608.951(1*C*)	11610.221(2*C*)
$\frac{2}{3}$	0.423	4	11607.998(0*D*)	11609.268(1*D*)	11610.538(2*D*)

energies. The results, assuming a magnetic field of 1.36 T, are tabulated in Table I.

For a photon energy that precisely matches a threshold, we expect an increase in the photodetachment cross section and a dip in the percentage of ions surviving detachment [2]. The spectroscopy is blurred by motional broadening effects, so each observed threshold has finite width and some thresholds are unresolved. We include labels in Figs. 2 and 3 to show the expected locations of the Zeeman thresholds as indicated in Table I. We cannot make strong claims about clear resolution of Zeeman structure; however, much of the structure in Fig. 2 is highly repeatable, particularly the 0D threshold. The results in Fig. 3 have a finer point spacing in the photon energy showing greater resolution. We note that the 0C and 0D thresholds are visible and that the fit to the data suggests a lower energy for the 1A threshold. In any case, we expect the $n = 0$ transitions to be the most prominent given that the Wigner law curve is steepest for energies just above the zero-field threshold [2,18]. We also note that the 0C transition appears stronger in the fit curve and the data than the 0D transition, which is consistent with the relative weights given in Table I.

We note that these results appear much different in several ways from those of our most recent spectroscopy at the lowest threshold of S^- [12]. First, the overall degree of detachment is much larger than in the previous experiment. This is to be anticipated, given that the O^- spin-orbit splitting is much smaller and that as a result, the O^- Boltzmann population has a much higher occupancy of the initial state. In the current experiment, this leads to a much higher signal-to-noise ratio and thus higher spectroscopic resolution. This experiment's magnetic field is also increased 36% over previous experiments. We believe that these technical changes have yielded the enhanced resolution of cyclotron and Zeeman structure in the photodetachment. Clearly, however, it would be desirable to have greater resolution of the Zeeman thresholds. Further improvements of this kind would facilitate additional tests of the Zeeman transition strengths of the type described in Refs. [4,11].

V. CONCLUSIONS

Frequency-domain spectra of photodetachment in a magnetic field at the lowest threshold from O^- were observed using π-polarized laser light. Theoretical fits to the data yield a threshold energy of 11607.575(28) cm^{-1}. This measurement is compatible with other values recommended by the photodetachment microscope method. A larger initial state population as well as an increased magnetic field have contributed to enhanced spectral resolution over previous experiments. As a result we detect repeatable cyclotron and Zeeman structure that is consistent with the BIL theoretical model. Future experiments will measure the relative Zeeman transition strengths.

ACKNOWLEDGMENTS

Acknowledgment is made to Davidson College as well as the donors of the American Chemical Society Petroleum Research Fund for partial support of this research.

[1] W. A. M. Blumberg *et al.*, Phys. Rev. Lett. **40**, 1320 (1978).
[2] W. A. M. Blumberg *et al.*, Phys. Rev. A **19**, 139 (1979).
[3] D. J. Larson and R. C. Stoneman, Phys. Rev. A **31**, 2210 (1985).
[4] R. E. Elmquist *et al.*, Phys. Rev. Lett. **58**, 333 (1987).
[5] H. F. Krause, Phys. Rev. Lett. **64**, 1725 (1990).
[6] C. H. Greene, Phys. Rev. A **36**, 4236 (1987).
[7] I. I. Fabrikant, Phys. Rev. A **43**, 258 (1991).
[8] O. H. Crawford, Phys. Rev. A **37**, 2432 (1988).
[9] J. N. Yukich *et al.*, Phys. Rev. A **55**, R3303 (1997).
[10] D. M. Pendergrast and J. N. Yukich, Phys. Rev. A **67**, 062721 (2003).
[11] A. K. Langworthy *et al.*, Phys. Rev. A **69**, 025401 (2004).
[12] J. E. Wells and J. N. Yukich, Phys. Rev. A **80**, 055403 (2009).
[13] L. D. Landau and E. M. Lifshitz, *Quantum Mechanics: Non-relativistic Theory* (Addison-Wesley, Reading, MA, 1991).
[14] L. G. Christophorou, *Electron-Molecule Interactions and Their Applications* (Academic Press, New York, 1984), Vol. 1.
[15] M. J. Travers *et al.*, Chem. Phys. Letters **164**, 449 (1989).
[16] C. Blondel *et al.*, Eur. Phys. J. D **33**, 335 (2005).
[17] C. Blondel *et al.*, Phys. Rev. A **64**, 052504 (2001).
[18] E. P. Wigner, Phys. Rev. **73**, 1002 (1948).